17th World Conference on Earthquake Engineering, 17WCEE

Sendai, Japan - September 13th to 18th 2020

A HYBRID BASE ISOLATION SYSTEM WITH MASS DAMPERS TUNED TO HIGHER MODE TO CONTROL SESIMIC ACCELERATIONS

Y. D. Shi[(1)], K. Saburi[(2)], M. Nakashima[(3)]

[(1)] *Associate Professor, Key Laboratory of Coast Civil Structure Safety of Ministry of Education, Tianjin University, China, yundong@tju.edu.cn*

[(2)] *Group leader, Design Department, Osaka Main Office, Takenaka Co., Ltd., Japan, saburi.kazuhiro@takenaka.co.jp*

[(3)] *President, Kobori Research Complex (KRC), Kajima Corporation, Japan, nakashima@archi.kyoto-u.ac.jp*

Abstract

Base isolation has been accepted as an effective method to protect structures and their contents during earthquakes. Recently, researchers are also developing three-dimensional (3D) base isolations which can further enhance the functionality of structures under vertical motions. Base isolation is developed to control the acceleration of the structure by isolating the superstructure from the ground with a long natural period. The long period generally results in small floor acceleration but causes large displacement at the base floor and rocking behavior for a 3D isolation. Typically, there are two approaches to control the displacement: shortening the natural period with relatively stiff isolators or increasing the base damping. However, both approaches increase the floor acceleration and consequently reduce the effectiveness of the base isolation because of the increased participation of higher modes, especially for high structures.

Previous researches have used tuned mass damper (TMD) to dissipate energy in an earthquake event, with the target to reduce the displacement of isolators by tuning the mass damper to the first mode of the base-isolated structure. In this study, a hybrid base isolation system with TMDs tuned to the higher modes is proposed with the target to reduce the floor accelerations in horizontally isolated and 3D isolated structures. A series of Matlab simulations are performed for steel frames with different heights to confirm the performance of the proposed TMD system. Both linear and nonlinear type isolations are evaluated in the simulation. Horizontally isolated and 3D isolated structures with different parameters for the structure and the isolators are investigated in the simulation.

The results show that a TMD tuned to the second mode of a horizontally base-isolated structure is generally more effective in reducing the roof acceleration than a TMD tuned to the first mode. The reduction ratio, defined as the maximum roof acceleration with the TMD relative to that without the TMD, is approximately 0.9 with the second-mode TMD for linear base isolation. The higher effectiveness of the second-mode TMD relative to the first-mode TMD is attributed primarily to the fact that the contribution of the second mode to the floor isolation is close to or even higher than that of the first mode in base-isolated structures. The larger TMD mass ratio and lower modal damping ratio of the second-mode TMD compared to the first-mode TMD increases its effect on modal acceleration reduction. For bilinear hoizontally base isolation, the first-mode period will change according to the base displacement. However, the second-mode period is controlled primarily by the superstructure and is relatively constant. The reduction ratio with the second-mode TMD improves to 0.8 for bilinear base isolation, while the first-mode TMD is ineffective because of the detuning effect caused by the change in the first-mode. Additionally, the displacement experienced by the second-mode TMD is considerably smaller than that of the first-mode TMD, thereby reducing the installation space for the TMD. For the 3D isolation, when the TMD is tuned to higher mode of the structure, the reduction ratio can also maintain at approximately 0.95-0.8 for linear base isolation while not causing significant rocking behavior.

Keywords: base isolation, tuned mass damper, rocking behavior, higher mode tuning, hybrid control

1. Introduction

Among the various techniques for enhancing the safety and functionality of structures subjected to earthquake excitation, base isolation is one of the most successful and widely applied techniques [1, 2]. Base isolation is developed to control the acceleration of the structure in an earthquake event by isolating the superstructure from the ground with a natural period that is much longer than the dominant periods of the ground motion. To date, the applications mainly focused on horizontal isolations. Recently, researchers are also developing three-dimensional (3D) base isolations which can further enhance the functionality of structures under vertical motions [3]. The differences between the traditional horizontal base isolation and the 3D isolation is that the 3D isolation can isolate the vertical vibrations. However, the vertical isolation normally does not help reduce horizontal acceleration and rocking behavior normally happens because of the coupling of the horizontal and vertical motions. A long natural period is preferred for both the horizontal and 3D isolations because it generally results in small floor acceleration but at the expense of large displacement at the base isolation floor. For the 3D isolation, a long natural period can cause more significant rocking behavior which can further increase the horizontal acceleration. Typically, there are two approaches to control the displacement of a base isolation floor: shortening the natural period with relatively stiff isolators or increasing the base damping. However, both approaches increase the floor acceleration and consequently reduce the effectiveness of the base isolation [4].

To control the acceleration of a base-isolated structure without causing a significant increase in displacement and rocking behavior, additional seismic control techniques or devices can be used. The tuned mass damper (TMD) is developed originally to mitigate the wind-induced vibrations of tall buildings. Extensive research has been conducted to determine the optimal design of TMDs, and numerous applications, particularly for wind response reduction, are found [5, 6]. Recently, the TMD system is explored for its application to seismic response reduction [7-9]. Most studies have focused on traditional fixed-base structures in which the TMD is generally tuned to the first-mode period of the structure. For example, Ref. [7] reported that the reduction ratio, defined as the maximum response (displacement or acceleration) with a TMD relative to the maximum response without a TMD, could be as high as 50% under the recorded ground motions of six- and ten-story structures with mass ratios of approximately 5%. Several studies have examined the application of TMDs to base isolation [10-12], but no practical application has been presented. In previous research, the TMD is mainly aimed at reducing the base displacement by tuning to the first mode of the base-isolated structure. In addition, the effectiveness of the suppression of the base displacement depended on the type of ground motion.

Thus far, there are limited research on the effectiveness of TMDs on the acceleration reduction of base-isolated structures, especially for 3D isolated structures. Compared with traditional low- to mid-rise fixed-base structures, base-isolated structures have a relatively longer first-mode period and higher base damping (potentially more than 15–20% to control the displacement). As the first-mode period of the base-isolated structure is designed to be much longer than the dominant periods of the ground motion, the first-mode response is not necessarily the primary source that generates the acceleration response. On the other hand, high base damping will promote the acceleration responses of higher modes in base-isolated structures compared to fixed-base structures. Because of these unique characteristics of base isolation compared to the fixed-base case, the traditional method of tuning the TMD to the first mode of a structure may not be effective for reducing earthquake-induced accelerations of base-isolated structures.

To improve the effectiveness of TMDs in reducing the floor acceleration of base-isolated structures, a second-mode TMD system has been proposed in which the TMD is tuned to the second-mode period of the isolated structure. Simulations are conducted to study the possibility of using TMDs in reducing the floor acceleration of horizontally isolated structures. Two types of damping, i.e., viscous damping and hysteretic damping, are considered for the dampers installed in the base isolation. Detail results and the theoretical model to explain the effectiveness of the second-mode TMD can be referred to Ref. [13]. In addition, a simplified model is established and a series of simulations are performed to further study the performance of a higher-mode tuned TMD in reducing the floor acceleration of 3D isolations in this paper. The 3D isolations are simulated with linear isolators, and different horizontal and vertical isolation period and height to width ratio of the structure are considered.

2. Multi-story base-isolated structure model

To examine the effectiveness of TMDs for reducing floor acceleration, an *n*-story base-isolated structure equipped with horizontal or 3D isolators and viscous dampers is considered as shown in Fig. 1. A TMD, represented by a linear spring and a viscous damper, is installed on the roof of the superstructure. For the horizontally isolated structure, the structure is modeled such that the mass is lumped at each floor level and the floors are displaced only laterally with no rotational movement. For the 3D isolated structure, the axial deformation of the columns and out of plane deformation of the slabs and beams are ignored. The whole structure can move vertically due to the flexibility of the 3D isolators in vertical direction. The rocking behavior of the structure is also simulated by considering a rotational angle at the base.

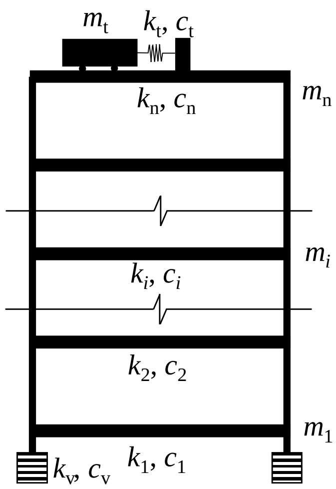

Fig. 1 – Multi-story base-isolated structure

2.1 Models for horizontally isolated structure

With the above assumptions, the equations of motion can be expressed in matrix form as follows:

$$\mathbf{M\ddot{x}} + \mathbf{C\dot{x}} + \mathbf{Kx} = -\mathbf{M1}\ddot{x}_g \tag{1}$$

where $\mathbf{x} = [x_1, x_2 \ldots x_n, x_t]$ is the floor displacement vector of the superstructure (x_1–x_n) and the TMD (x_t) relative to the ground; **1** is a unit vector; $\ddot{x}_g$ is the absolute horizontal ground acceleration; and **M**, **C,** and **K** are the mass, damping, and stiffness matrices of the system, respectively.

The damping matrix of the superstructure is considered proportional to the superstructure's stiffness matrix when ignoring the TMD and base isolators:

$$\mathbf{C}_{sup} = \frac{2\zeta_{sup}}{\omega_{sup}}\mathbf{K}_{sup},\ \mathbf{K}_{sup} = \begin{bmatrix} k_2 & -k_2 & & \\ -k_2 & k_2+k_3 & -k_3 & \\ & -k_3 & \ddots & \ddots \\ & & \ddots & k_n \end{bmatrix},\ \mathbf{C}_{sup} = \begin{bmatrix} c_2 & -c_2 & & \\ -c_2 & c_2+c_3 & -c_3 & \\ & -c_3 & \ddots & \ddots \\ & & \ddots & c_n \end{bmatrix} \tag{2}$$

where k_i and c_i are the stiffness and damping coefficients of the *i*th superstructure's floor; ω_{sup} is the fundamental circular frequency of the superstructure when the base is fixed without TMD, and ζ_{sup} is the corresponding damping ratio.

2.2 Models for 3D isolated structure

For the 3D isolated structure, two new parameters are introduced to describe the movement of the structure in the vertical direction and the rocking behavior. With the above assumptions, the equations of motion can be expressed in matrix form as follows:

$$\mathbf{M}_{3D}\ddot{\mathbf{U}}_{3D} + \mathbf{C}_{3D}\dot{\mathbf{U}}_{3D} + \mathbf{K}_{3D}\mathbf{U}_{3D} = -\mathbf{M}_{3D}\mathbf{N}_{3D}\ddot{\mathbf{U}}_{\mathbf{g}} \tag{3}$$

where $\mathbf{U} = [U_{x1}, U_{x2}\ldots U_{xn}, U_{xt}, U_z, U_\theta]$; U_{x1}–U_{xn} are the horizontal floor displacements of the superstructure and U_{xt} is the horizontal displacement of the TMD; U_z and U_θ are the vertical displacement of the whole structure and the rotational angle of the structure a the isolation layer. All the U values are calculated relative to the ground. $\ddot{U}_g = [\ddot{U}_{gx}, \ddot{U}_{gz}]$ is the absolute horizontal and vertical ground acceleration vector. The other matrices are as follows:

$$\mathbf{M}_{3D} = \begin{pmatrix} m_1 &&&&&&&& \\ & m_2 &&&&&&& \\ && \ddots &&&&&& \\ &&& m_i &&&&& \\ &&&& \ddots &&&& \\ &&&&& m_n &&& \\ &&&&&& m_t && \\ &&&&&&& \sum_{i=1}^{n} m_i + m_t & \\ 0 & hm_2 & \cdots & (i-1)hm_i & \cdots & (n-1)hm_n & (n-1)hm_t & 0 & \frac{1}{12}\sum_{i=1}^{n} m_i b^2 \end{pmatrix}$$

$$\mathbf{K}_{3D} = \begin{pmatrix} k_1+k_2 & -k_2 &&&&&&& k_2 h \\ -k_2 & k_2+k_3 & -k_3 &&&&&& (k_3-k_2)h \\ & \ddots & \ddots & \ddots &&&&& \vdots \\ && -k_i & k_i+k_{i+1} & -k_{i+1} &&&& (k_{i+1}-k_i)h \\ &&& \ddots & \ddots & \ddots &&& \vdots \\ &&&& -k_n & k_n+k_t & -k_t && -k_n h \\ &&&&& -k_t & k_t & 0 & 0 \\ &&&&&& 0 & k_z & 0 \\ &&&&&&& 0 & k_z b^2/4 \end{pmatrix}$$

$$\mathbf{C}_{3D} = \begin{pmatrix} c_1+c_2 & -c_2 &&&&&&& c_2 h \\ -c_2 & c_2+c_3 & -c_3 &&&&&& (c_3-c_2)h \\ & \ddots & \ddots & \ddots &&&&& \vdots \\ && -c_i & c_i+c_{i+1} & -c_{i+1} &&&& (c_{i+1}-c_i)h \\ &&& \ddots & \ddots & \ddots &&& \vdots \\ &&&& -c_n & c_n+c_t & -c_t && c_n h \\ &&&&& -c_t & c_t & 0 & 0 \\ &&&&&& 0 & c_z & 0 \\ &&&&&&& 0 & c_z b^2/4 \end{pmatrix}$$

$$\mathbf{N}_{3D} = \begin{bmatrix} m_1 & 0 \\ \vdots & \vdots \\ m_i & 0 \\ \vdots & \vdots \\ m_n & 0 \\ m_t & 0 \\ 0 & \sum_{i=1}^{n} m_i + m_t \\ \sum_{i=2}^{n}(i-1)hm_i + (n-1)hm_t & 0 \end{bmatrix}$$

where m_i is the mass of each floor of the ith floor of the superstructure; k_z and c_z are the stiffness and damping coefficients of the vertical isolation; h and b are the height of each story and width of the structure.

2.3 Model parameters

Three base-isolated prototypes of different heights (5-, 10- and 15-story) with superstructures made of steel are considered (Table 1). The detail designs of the structures can be found in Ref. [13]. Assuming that the superstructure is rigid, Case I and Case II represent base-isolated structures with a horizontal natural period 2.5 and 3.5 times the first-mode period of the superstructure, respectively. The base damping is adjusted by trial and error to ensure that the maximum displacement would reach 250 mm. As a result, Case II requires smaller stiffness and higher damping than Case I to achieve the same maximum base displacement. Notably, the second-mode periods of the two cases (see T_2 in Table I) are similar, indicating that the second mode of the base-isolated structure is controlled primarily by the vibrational characteristics of the superstructure.

For the 3D isolated structure, the damping for the vertical isolation layer ξ_{bz} is assumed to be 20%. For both the horizontally and 3D isolated structures, the TMD is installed on the roof. The mass ratio, defined as the ratio of the TMD mass to the total mass of the structure, and the damping for the TMD are selected as 5% and 10%, respectively [11, 13].

Table 1 – Base-isolated structures for simulation

	5-story		10-story		15-story	
m(x10^3 kg)	m_1~ m_4: 981, m_5: 1472		m_1~ m_9: 981, m_{10}: 1472		m_1~ m_{14}: 981, m_{15}: 1472	
$k_{2\sim i}$ (kN/m)	k_2: 1030050, k_3: 931950 k_4: 735750, k_5: 53955		k_2: 1471500, k_3: 1275300 k_4: 1226250, k_5: 1128150 k_6: 1030050, k_7: 931950 k_8: 784800, k_9: 637650 k_{10}: 784800		k_2: 1912950, k_3: 1863900 k_4: 1814850, k_5: 1716750 k_6: 1667700, k_7: 1569600 k_8: 1520550, k_9: 1422450 k_{10}: 1275300, k_{11}: 1177200 k_{12}: 1030050, k_{13}: 882900 k_{14}: 686700, k_{15}: 490500	
ζ_{sup}	2%		2%		2%	
	Case I	Case II	Case I	Case II	Case I	Case II

k_1 (kN/m)	74600	38260	45130	23540	42180	21580
ξ_{bx}	7%	17%	20%	28%	25%	43%
T_1 (s)	1.79	2.43	3.18	4.28	4.00	5.44
T_2 (s)	0.38	0.39	0.67	0.68	0.83	0.85
ξ_{bz}	20%	20%	20%	20%	20%	20%

T_1 and T_2 are the first- and second-mode periods of the base-isolated structure.

3. Simulations for horizontally isolated structure

3.1 Ground motions

To evaluate the effectiveness of higher mode tuning of the TMD in reducing the responses of base-isolated structures to real earthquake motion, a suite of 80 recorded ground motions is selected. The ground motions are gathered for the PEER Transportation Systems Research Program (TSRP) [14]. The TSRP has several groups of motions, each group containing a set of 40 three-component ground motions. The motions used for this study are chosen from the fault normal and vertical (for 3D isolated structure simulation) component of broad-band ground motions with rock and soil site conditions. All ground motions are amplitude-scaled to have a PGV of 0.5 m/s to match the design response spectrum in the Japanese code [15]. Fig. 2 shows the acceleration response spectra for the scaled motions. As shown in the figures, the amplitudes of the ground motion spectra for the rock site condition (Fig. 2(a)) are smaller than those for the soil site condition (Fig. 2 (b)) in the long period band due to the site filtering effect.

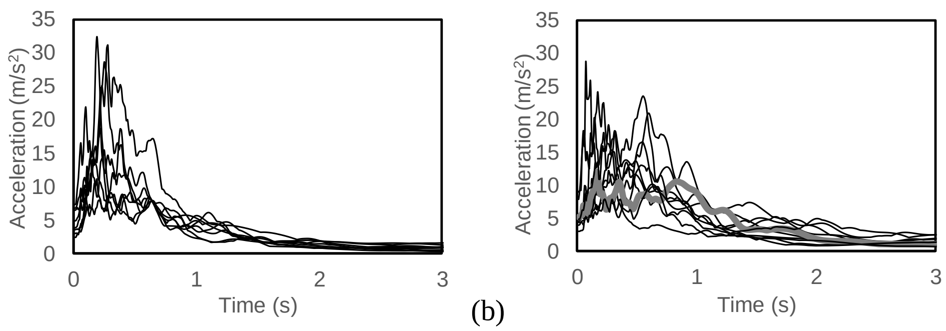

Fig. 2 – Acceleration spectra for 80 recorded ground motions (5% damping): (a) rock site; (b) soil site

3.2 Simulations for linear isolators

The three horizontally isolated prototypes are used in the simulation. The TMDs are tuned to two periods, which correspondes to the first two modes of the base-isolated structures. The results for Case II (as shown in Table 1) are shown in Fig.3 for the reduction ratio, defined as the roof acceleration with the TMD normalized by the value without the TMD.

For Case II isolations with relatively higher base damping and longer period than Case I, the second-mode TMD is more effective than the first-mode TMD for all three structures under the ground motions with both rock and soil site conditions. Under ground motion with soil site condition, the mean values of the reduction ratios of the roof accelerations are 0.93, 0.86, and 0.86 for the 5-, 10-, and 15-story base-isolated structures with their TMD tuned to the second mode. When the TMD is tuned to the first mode, the mean values are 0.94, 0.98, and 0.99 for the three base-isolated structures, which indicates that first-mode tuning has no effect on the reduction of the roof acceleration. Tuning to the second mode is more effective by approximately 6% for the 10- and 15-story base-isolated structures than for the 5-story base-isolated structures. The TMD reduces the roof acceleration (ratio smaller than 1) for most of the ground motions, as shown in Fig. 3. Under ground motion with rock site condition, the mean reduction ratios of the floor response are 0.85, 0.88, and 0.87 for the 5-, 10-, and 15-story base-isolated structures with the TMD tuned to the second mode. When the TMD is tuned to the first mode, the mean reduction ratios are 0.97, 0.99, and 0.99 for the three base-isolated structures. The advantage of the second-mode TMD for the 5-story isolation is more apparent under ground motions with rock site condition than with soil site condition because the second mode's contribution increases with rock site condition. In summary, with the second-mode TMD, the reduction ratio of the roof acceleration is approximately 0.9 for the recorded ground motions.

The reason to have a higher efficiency in controlling the roof acceleration by the second-mode TMD is that the modal damping of the second mode is commonly lower than that of the first mode in base isolation, due to relatively high base damping. In addition, the equivalent mass ratio of the second-mode TMD is larger than that of the first-mode TMD. These two characteristics result in higher efficiency of the second-mode TMD in reducing the modal response as explained in Ref. [13]. In addition, as the base isolation generally has a relatively long first-mode period and high base damping, the contribution of the modal response of the second mode to the roof acceleration is close to or even higher than that of the first mode, especially for taller structures. Hence, the second-mode TMD reduces roof acceleration more effectively.

There are few cases in which the reduction ratio is larger than one indicating the amplification of floor accelerations by the second-mode TMD because the frequency components are more dominant around the two newly created modes with the adding TMD than around the second mode of the structure without the TMD, resulting in larger accelerations. The simulation also shows that for the 80 motions, a 15% error in the tuned period for the second-mode TMD would not affect the control efficiency.

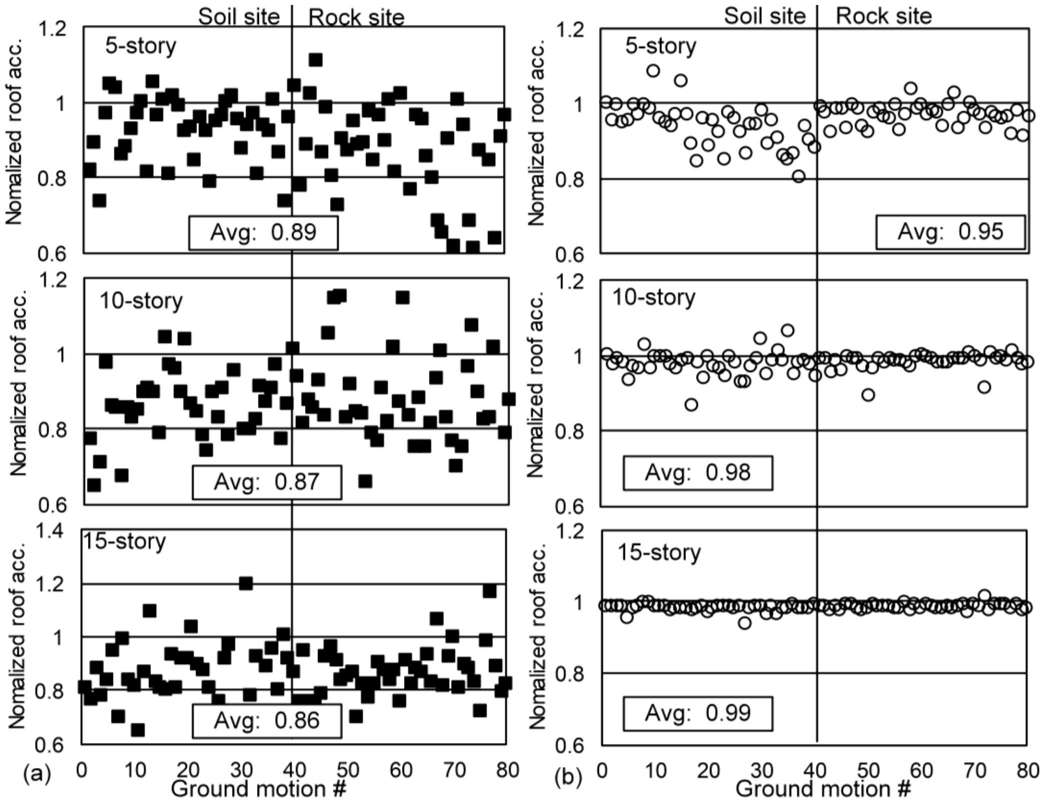

Fig. 3 – Normalized roof acceleration for Case II of horizontally isolated structure: (a) second-mode TMD; (b) first-mode TMD

3.3 Simulations for bilinear isolators

To check the efficiency of TMD for nonlinear isolation, the prototypes designed in Table 1 are modified by a bilinear stiffness model as shown in Fig. 4. The parameters k_1, k_2, and Q are estimated to adjust the equivalent stiffness k_{eq} and equivalent damping ratio ξ_{eq} to be identical with the values for the linear base isolation defined in Table 1, for a given maximum displacement d_{eq}. As the selection of d_{eq} affects the stiffness of the isolation, two values (d_{eq} = 100 mm and 200 mm) are adopted for comparison. Note that the mean maximum displacement of the linear base isolation under the ground motions with soil and rock conditions for all the three structures is 197 mm. Table 2 presents the design parameters of the isolations.

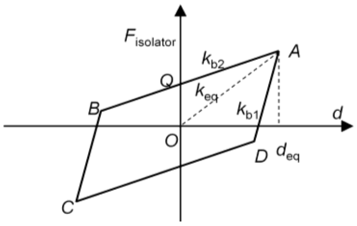

Fig. 4 – Bilinear model for isolators

Table 2 – Bilinear base isolations

d_{eq}	Parameters	5-story		10-story		15-story	
		Case I	Case II	Case I	Case II	Case I	Case II
200 mm	k_1 (x 10^6 kN/m)	134.4	111.9	147.0	97.8	161.1	125.9
	k_2 (x 10^6 kN/m)	66.4	27.0	29.3	11.8	23.5	4.9
	Q_1 (x 10^6 kN)	1.9	2.4	3.3	2.4	3.9	3.4
100 mm	k_1 (x 10^6 kN/m)	105.2	75.4	96.5	60.9	102.1	73.9
	k_2 (x 10^6 kN/m)	64.4	24.6	26.0	9.4	19.6	1.5
	Q_1 (x 10^6 kN)	1.2	1.4	2.0	1.5	2.3	2.1

Fig. 5 graphically shows the reduction ratios. They are all around 0.8 for the second-mode TMD for the three structures. Compared with the linear base isolation, where the mean reduction ratio is around 0.9, the TMD for bilinear base isolation is more efficient. This is deemed attributed primarily to the increased contribution of the second mode to the total response in the bilinear base isolation.

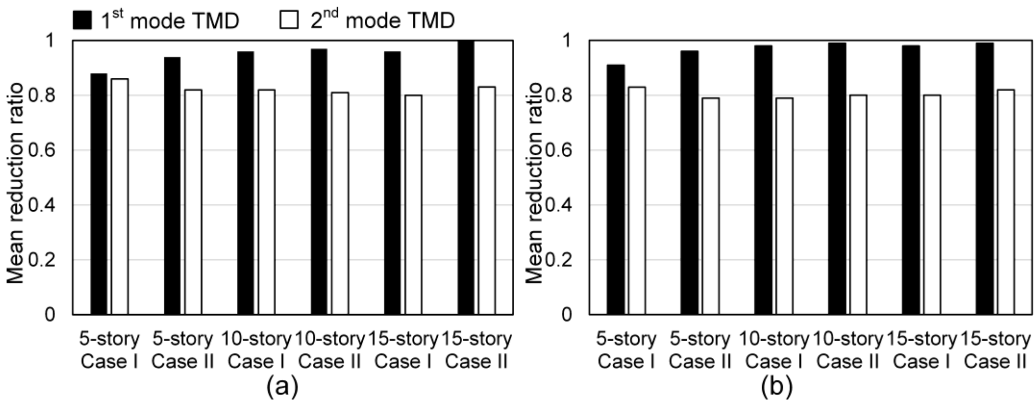

Fig. 5 – Mean reduction ratios of bilinear structures with different displacement corresponding to the calculation of the equivalent stiffness: (a) d_{eq}=100 mm; (b) d_{eq}=200 mm

4. Simulations for 3D isolated structure

4.1 Vibration mode

The three 3D isolated structures with different height are selected for simulation. When the vertical isolation is installed, rocking behavior will happen with different parameters of the structure and isolation periods due to the coupling effect of horizontal and vertical movements. Normally, a relatively longer isolation period both in horizontal and vertical directions is preferred in order to more effectively control the floor acceleration [3]. Table 3 gives the mode period of the 3D isolated structures. Two different horizontal to vertical isolation period ratios T_x/T_z and two height to width ratios H/b of the structure are considered.

As shown in the table, the first two periods are significantly influenced by the T_x/T_z and H/b parameters. Unlike the horizontally isolated structures, the second mode period of the 3D isolated structures changes with respect to different conditions. A smaller horizontal isolation period to vertical isolation period ratio T_x/T_z and larger height to width ratio H/b of the structure will generate more significant rocking behavior and elongate the isolation period of the corresponding horizontal isolations. However, the higher mode remains relatively constant because it is primarily controlled by the superstructure's characteristics.

Table 3 – Mode period of the 3D isolated structures (unit: s)

				1st mode	2nd mode	3rd mode	4th mode
5-story	Case I	T_x/T_z=6	H/b=3	2.06	0.54	0.28 (z)	0.21
		T_x/T_z=4		2.38	0.64	0.43 (z)	0.21
	Case II	T_x/T_z=6		2.95	0.68	0.40 (z)	0.21
		T_x/T_z=4		3.50	0.81	0.60 (z)	0.21
10-story	Case I	T_x/T_z=6		3.77	0.95	0.50 (z)	0.37
		T_x/T_z=4		4.43	1.10	0.76 (z)	0.37
	Case II	T_x/T_z=6		5.31	1.15	0.69 (z)	0.37
		T_x/T_z=4		6.43	1.35	1.04 (z)	0.37
	Case I	T_x/T_z=6	H/b=5	4.64	1.11	0.50 (z)	0.37
		T_x/T_z=4		6.09	1.23	0.76 (z)	0.37
	Case II	T_x/T_z=6		6.81	1.36	0.69 (z)	0.37
		T_x/T_z=4		9.14	1.49	1.04 (z)	0.37
15-story	Case I	T_x/T_z=6	H/b=3	5.93	1.04	0.64 (z)	0.46
		T_x/T_z=4		7.63	1.10	0.95 (z)	0.46
	Case II	T_x/T_z=6		9.36	1.15	0.88 (z)	0.46
		T_x/T_z=4		12.68	1.32 (z)	1.22	0.46

(z) indicates the vertical mode;

4.2 Simulation results

In order to verify the effectiveness of higher mode TMD in reducing the roof acceleration, different schemes are investigated. Figs. 6 and 7 show the roof acceleration reduction ratio by tuning the TMD to the first mode, second mode (the third mode for the last simulation case in Table 3) and fourth mode, respectively.

For Case I isolations (Fig. 6) with relatively lower base damping and shorter isolation period, the mean values of the reduction ratios of the roof accelerations are 0.94, 0.87, and 0.81 for the 5-, 10-, and 15-story 3D isolated structures with their TMD tuned to the fourth mode. When the TMD is tuned to the second mode (third mode TMD for the last simulation case in Table 3), the mean values are 0.91, 0.93, and 0.93 for the three 3D isolated structures. When the TMD is tuned to the first mode, the mean values are 0.89, 0.96, and 0.99. Tuning to the fourth mode is more effective by 6%-18% for the 10- and 15-story 3D isolated structures comparing to other two schemes. The TMD reduces the roof acceleration (ratio smaller than 1) for most of the ground motions, as shown in Fig. 6. For the 5-story case, the first-mode tuning is more effective. This is similar with the findings for the horizontally isolated structures [13]. When the isolation period is elongated and the damping is increased in Case II (Fig. 7), the effectiveness of the fourth-mode TMD is further promoted because the modal damping of the first and second mode is higher and the equivalent mass ratio of these two modes is smaller. The mean values of the reduction ratios of the roof accelerations are 0.93, 0.83, and 0.78 for the 5-, 10-, and 15-story 3D isolated structures with their TMD tuned to the fourth mode. When the TMD is tuned to the second mode (third mode TMD for the last simulation case in Table 3), the mean values are 0.94, 0.95, and 0.94 for the three 3D isolated structures. When the TMD is tuned to the first mode, the mean values are 0.93, 0.98, and 1.00.

It is worth to note that tuning the TMD to the fourth mode only causes a slight change of the rotation angle by ±3% for the 10- and 15-story 3D isolated structures. Also, a higher mode tuning scheme will significantly reduce the displacement of the TMD which is beneficial for the installation of the TMD. When the TMD is tuned to the first mode, it reduces the rotation angle by 5%-15%; thus, it is reasonable to tune the TMD to the first when the control target is the to reduce the rotation angle.

When the horizontal isolation period to vertical isolation period ratio T_x/T_z and height to width ratio H/b of the structure vary, the control efficiency remains similar as shown in Figs. 8 and 9. The change of those two parameters mainly affect the rocking behavior of the structure. The results show that the higher-mode TMD scheme is also effective when rocking behavior varies in the 3D isolated structure.

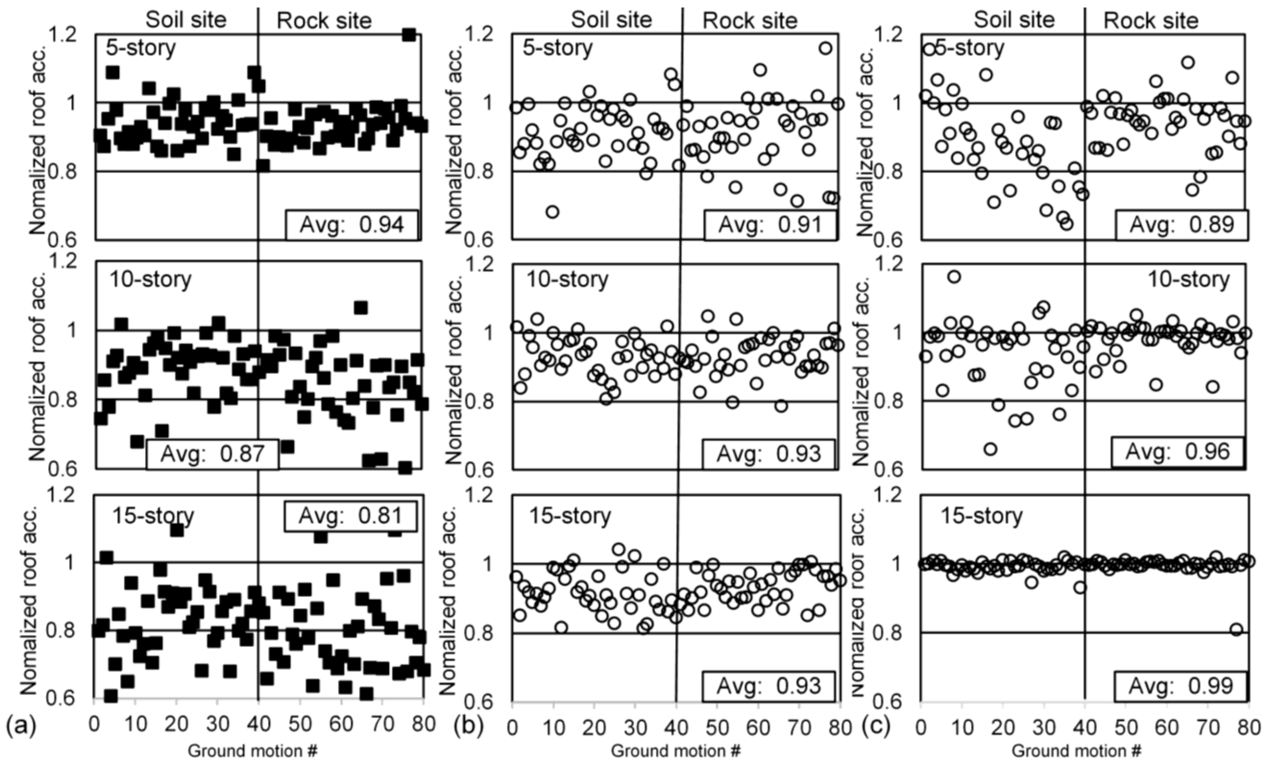

Fig. 6 – Normalized roof acceleration for Case I with T_x/T_z=4 and H/b=3: (a) fourth mode TMD; (b) seond mode TMD (third mode TMD for the last simulation case in Table 3); (c) first mode TMD

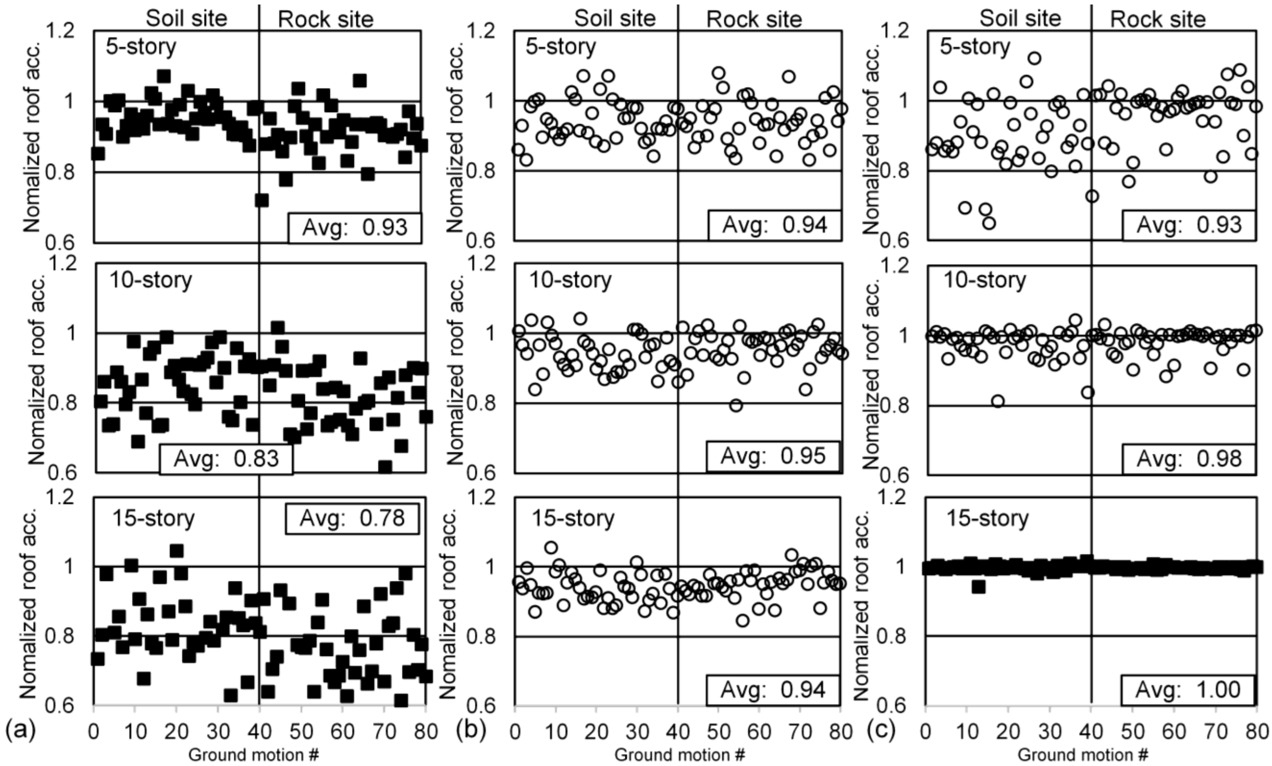

Fig. 7 – Normalized roof acceleration for Case II with T_x/T_z=4 and H/b=3: (a) fourth mode TMD; (b) seond mode TMD (third mode TMD for the last simulation case in Table 3); (c) first mode TMD

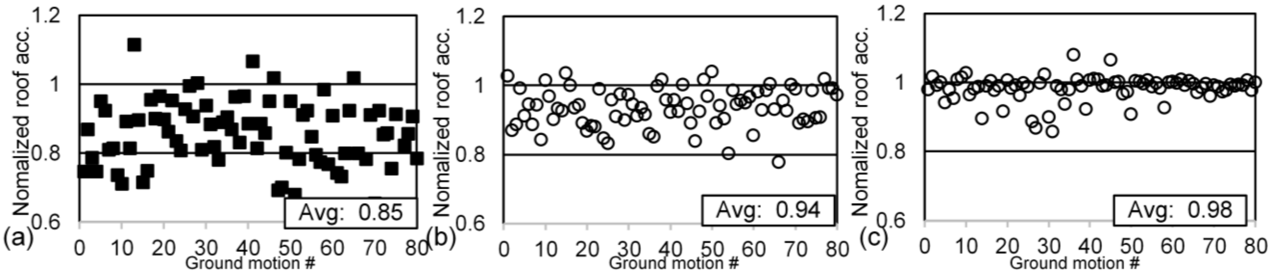

Fig. 8 – Normalized roof acceleration for Case II with T_x/T_z=6 and H/b=3: (a) fourth mode TMD; (b) seond mode TMD (third mode TMD for the last simulation case in Table 3); (c) first mode TMD

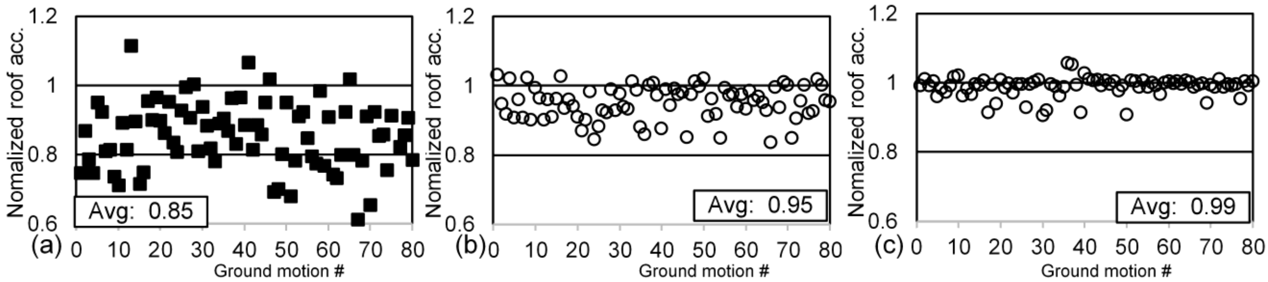

Fig. 9 – Normalized roof acceleration for Case II with T_x/T_z=4 and H/b=5: (a) fourth mode TMD; (b) seond mode TMD (third mode TMD for the last simulation case in Table 3); (c) first mode TMD

5. Conclusion

The application of TMD to reduce the seismic floor acceleration of horizontally and 3D isolated structures is investigated. The major findings are summarized as follows:

(1) For a horizontally isolated structure, a TMD tuned to the second mode of the isolated structure is generally more effective in reducing the roof acceleration than a TMD tuned to the first mode, due to the lower modal damping and larger equivalent mass ratio of the second mode. The floor acceleration reduction ratio is approximately 0.9 with the second-mode TMD for linear isolation and 0.8 for bilinear isolation.

(2) For a 3D isolated structure, it is not effective for the 3D isolated structure to use the second-mode TMD as the second mode of the 3D isolated structure is significantly affect by the coupling effect of the horizontal and vertical isolation movement. Tuning to the third mode of the structure (except considering the vertical mode which is independent as shown in Eq. (3)) is more effective, and generally the acceleration reduction ratio is about 0.95-0.8.

6. Acknowledgements

The authors gratefully acknowledge the support for this research from the National Natural Science Foundation of China under grant No. 51978463.

7. References

[1] Sato E, Furukawa S, Kakehi A, Nakashima M (2011): Full shaking table test for examination of safety and functionality of base-isolated medical facilities. *Earthquake Engineering and Structural Dynamics*, **40**, 1435-1453.

[2] Shi Y, Kurata M, Nakashima M (2014): Disorder and damage of base-isolated medical facilities when subjected to near-fault and long-period ground motions. *Earthquake Engineering and Structural Dynamics*, **43**(11),1683-1701.

[3] Chen Z, Ding Y, Shi Y, Li Z (2019): Research on isolation performance of three dimensional isolation device with variable stiffness for long span spatial structures. *Building Structures*, **40(10)**, 28-35.

[4] Kelly JM (1999): The role of damping in seismic isolation. *Earthquake Engineering and Structural Dynamics*, **28**, 3-20.

[5] Den Hartog JP (1956): *Mechanical Vibrations*, Mc Graw-Hill: New York.

[6] Holmes D (1995): Listing of installations. *Engineering Structures*; **17**, 676–678.

[7] Sadek F, Mohraz B, Taylor AW, Chung RM (1997): A method of estimating the parameters of tuned mass dampers for seismic applications. *Earthquake Engineering and Structural Dynamics*, **26**, 617-635.

[8] Moutinho C (2012): An alternative methodology for designing tuned mass dampers to reduce seismic vibrations in building structures. *Earthquake Engineering and Structural Dynamics*, **41**(14), 2059-2073.

[9] Pinkaew T, Lukkunaprasit P, Chatupote P (2003): Seismic effectiveness of tuned mass dampers for damage reduction of structures. *Engineering Structures*, **25**, 39-46.

[10] Palazzo B, Petti L, Ligio MD (1997): Response of base isolated systems equipped with tuned mass dampers to random excitations. Journal of structural control, **4**, 9-22.

[11] Taniguchi T, Kiureghian AD, Melkumyan M (2008): Effect of tuned mass damper on displacement demand of base-isolated structures. *Engineering Structures*, **30**, 3478-3488.

[12] Domenico D, Ricciardi G (2018): An enhanced base isolation system equipped with optimal tuned mass damper inerter (TMDI). *Earthquake Engineering and Structural Dynamics*, **47**,1169–1192.

[13] Shi Y, Saburi K, Nakashima M (2018): Second-mode tuned mass dampers in base - isolated structures for reduction of floor acceleration. *Earthquake Engineering and Structural Dynamics*, **47**(12), 2519-2538.

[14] Japanese Ministry of Construction (2000): Notification No. 1461-2000: *Stipulation of criteria for structural calculations performed to confirm the safety from the perspective of structural capacity of high-rise buildings*. MC, Japan. (in Japanese)

[15] Baker JW, Lin T, Shahi SK, Jayaram N (2011): New ground motion selection procedures and selected motions for the PEER transportation research program, *Report No. PEER11/03*, Pacific Earthquake Engineering Research Center, University of California, Berkeley, CA.

